EPSC Abstracts
Vol. 5, EPSC2010-204, 2010
European Planetary Science Congress 2010

The shape and physical properties of asteroid 2867 Steins from OSIRIS images

P. Lamy (1), L. Jorda (1), S. Spjuth (2), S. Besse (1), S. Marchi (3), C. Barbieri (3), R. Gaskell (4), O. Groussin (1), M. Kaasalainen (5) and H. U. Keller (2)
(1) Laboratoire d'Astrophysique de Marseille, Université de Provence & CNRS, Marseille, France, (2) Max-Planck-Institut für Sonnensystemforschung, Katlenburg-Lindau, Germany (3) Department of Astronomy, University of Padova, Italy, (4) Planetary Science Institute, Tucson, USA, (5) Tampere University of Technology, Tampere, Finland
(philippe.lamy@oamp.fr / Fax: +33-491661855)

Abstract

The Rosetta spacecraft of the European Space Agency flew by the E-type asteroid 2867 Steins on 5 September 2008 on its way to its final target, comet 67P/Churyumov-Gerasimenko. We report here on a overall analysis and interpretation of the images of the asteroid acquired by OSIRIS, the imaging system aboard the spacecraft: shape and global physical properties, photometric properties of the surface, crater properties and age.

1. Introduction

The flyby of asteroid 2867 Steins by the Rosetta spacecraft took place on 5 September 2008 at a relative velocity of 8.6 km s^{-1}. Closest approach (CA) took place at 18:38:20 UTC at a distance of 803 km. During the approach, the solar phase angle was constant and equal to $38°$. It decreased to a minimum of $0.36°$ and increased thereafter to reach $51°$ at CA and finally $141°$ on the outbound trajectory. The asteroid was imaged through a variety of filters (from the ultra-violet to the near infra-red) by both the Narrow Angle Camera (NAC) and the Wide Angle Camera (WAC) of the "OSIRIS" Optical Spectroscopic and Infrared Remote Imaging System [7] aboard the spacecraft. The NAC observations unfortunately stopped 10 minutes before CA at a distance of 5200 km and a phase angle of $30°$. The last image of the NAC has a scale of 98 meters per pixel (m/pix), and the asteroid extends over 59 CCD pixels. The WAC acquired resolved images of the asteroid from ten minutes before CA to three minutes after. Images at closest approach have a scale of 81 m/pix and the body extends over 68 pixels.

2. Shape and global physical properties of Steins

Several methods were combined to retrieve the shape of the asteroid [6]: the "limb method", control points calculated by matching points of interest on several images by stereo [1], and stereophotoclinometry [2] to finally calculate the topography of the surface. The part of the asteroid which has not been observed during the flyby was constrained by inversion of a large set of light curves [8].

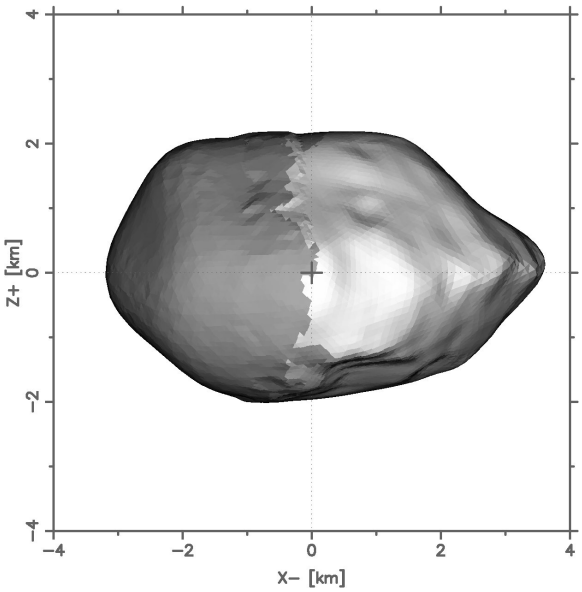

Figure 1: Final shape model of Steins. The equatorial ridge (right) and the crater Ruby (bottom) are the most prominent surface features. The dark area has been constrained by the lightcurve inversion technique.

The shape model has dimensions measured along the principal axes of inertia of $6.82 \times 5.70 \times 4.42$ km

and the radius of a sphere of equivalent volume amounts to $2.63\ \mathrm{km}$. The spin axis is directed towards $(\mathrm{RA}, \mathrm{Dec}) = (99 \pm 5^\circ, -59 \pm 5^\circ)$. The data make it possible to derive gravitational slopes and heights on the well-imaged portion of the asteroid following the method developed by Werner and Scheeres [9]. The most prominent topographic features are the large crater Ruby in the southern hemisphere and a ridge of 90° length in longitude located almost exactly at the equator (Fig. 1). The latter is likely due to partial reshaping by the Yarkovsky-O'Keefe-Radzievskii-Paddack (YORP) effect [5]. A "cliff" of $\sim 2000\ \mathrm{m}$ in length and $120 - 150\ \mathrm{m}$ in height is also observed in the northern hemisphere.

3. Photometric properties of Steins

The photometric properties of asteroid Steins were studied from the disk-resolved multi-spectral images obtained with the OSIRIS Wide Angle Camera (WAC) using Hapke[3, 4]'s formalism together with the above shape model composed of 2800 triangular facets. For a given image, we calculated the bi-directional reflectance (BDR) of each facet from the total flux received by the pixel(s) intersected by each facet. Our results suggest that the surface photometry of Steins shows both a Shadow-Hiding Opposition Effect (SHOE) and a Coherent-Backscatter Opposition Effect (CBOE). Opposition data are sensitive to surface porosity and grain size. The regolith of Steins appears to be porous, consisting of transparent fine grained particles. The modeled mean roughness slope angle is 26° and the single scattering albedo is 0.55, the highest ever observed for a small body in the solar system. The high albedo is probably associated with an iron-poor surface composition such as that of aubrite meteorites which are suspected to originate from the E-type asteroids. The geometric albedo was modeled with the Hapke parameters (Ap = 0.41) as well as measured directly from the image at opposition (Ap = 0.39). We found no photometric variations on the surface.

4. Crater properties and age of Steins

We have identified 42 craters on 44% of the surface whose diameters range from 150 to 2100 meters. Craters are more numerous on the western hemisphere, this is mainly due to the history of the surface itself. The cratering history was investigated by applying current models describing the formation and evolution of main belt asteroids that provide the rate and velocity distributions of impactors. These models coupled with appropriate crater scaling laws, allow the cratering history to be estimated. The cratering retention age of Steins, that is the time lapsed since its formation or global surface reset spans from a few hundred Myrs to more than 1 Gyr, depending on the adopted scaling law and asteroid physical parameters. Moreover, a marked lack of craters smaller than about 600 meters was found and interpreted as a result of a peculiar evolution of Steins cratering record, possibly related either to the formation of the 2.1 km wide impact crater near the south pole or to YORP reshaping. The physical properties of the craters were accurately calculated by a novel forward modeling technique which fits a model of an hemispherical crater to the images using the shape model described above of the body and the measured bidirectional reflectance. The depth-to-diameter ratio varies from 0.05 to 0.25. Shallow craters are present all over the observed surface and may be the result of regolith blanketing and/or a lack of raised crater rim. Deep craters are numerous on the surface and associated with fresh features, a result consistent with the relative young age of Steins. The deepest craters are deeper than the fresh craters found on previous asteroids (e.g 0.08 for Itokawa and 0.15 for Gaspra).

References

[1] Besse, S. 2009, PhD dissertation, Université de Provence

[2] Gaskell, R. W., and 15 colleagues 2008, Meteoritics and Planet. Sci. 43, 1049

[3] Hapke, B. 1986, Icarus 67, 264

[4] Hapke, B. 2002, Icarus 157, 523

[5] Harris, A. W., Fahnestock, E. G. and Pravec, P. 2009, Icarus 199, 310

[6] Jorda, L., Lamy, P., Groussin, O. et al. 2010, Icarus, in preparation

[7] Keller, H. U., Barbieri, C., Lamy, P. et al. 2007, Space Sci. Rev. 128, 433

[8] Lamy, P., Kaasalainen, M., Lowry, S. et al. 2008, A&A 487, 1179

[9] Werner, R. A. and Scheeres, D. J. 1996, Celest. Mech. 65, 313